IOP Conference Series: Earth and Environmental Science

PAPER • OPEN ACCESS

Measurement-driven AA-CAES Model for Distribution Network Dispatch in Coordination with Renewable Generation

To cite this article: Yuguang Xie *et al* 2020 *IOP Conf. Ser.: Earth Environ. Sci.* **529** 012006

IOP Conf. Series: Earth and Environmental Science **529** (2020) 012006 doi:10.1088/1755-1315/529/1/012006

Measurement-driven AA-CAES Model for Distribution Network Dispatch in Coordination with Renewable Generation

Yuguang Xie[1], Jiayu Bai[2,*], Dangwu Liu[3], Tianwen Zheng[4], Shengwei Mei[2]

[1] State Grid Anhui Electric Power Research Institute, Hefei 230601, China
[2] State Key Lab of Control and Simulation of Power Systems and Generation Equipments (Dept. of Electrical Engineering), Tsinghua University, Beijing 100084, China
[3] State Grid Anhui Electric Power CO., LTD., Hefei 230022, China
[4] Sichuan Energy Internet Research Institute, Tsinghua University, Chengdu 610213, China

*Email: bai_jiayu01@163.com

Abstract. Advanced adiabatic compressed air energy storage (AA-CAES) could play an important role in power distribution system for mitigating the intermittency of distributed renewable generations and reducing the peak-valley difference of load demand, which requires to operate AA-CAES under off-design conditions. A power system dispatch oriented AA-CAES model was proposed based on the technically thermodynamic performance curves of compressor and expansion calibrated from experiments, highlighting the impact of AA-CAES part-lard features on charging/discharging efficiency and capacity. The proposed model is integrated with economic dispatch problem of power distribution systems, giving rise to a nonlinear program due to the state-dependent charging and discharging performances. The dispatch model is further linearized via piecewise linear approximation and special-ordered set of type 2, and its equivalent mixed integer linear formulation is presented. A modified IEEE 33-bus system is adopted to verify the effectiveness of proposed model for renewables accommodation.

1. Introduction

Renewable generation is progressed rapidly and has been widely penetrated in power system to meet the challenge of energy crisis. Energy storage is taken as the most flexible supporting facility to cope with the intermittent supply and non-dispatchable features of renewables [1], among which compressed air energy storage (CAES), especially advanced adiabatic compressed air energy storage (AA-CAES) has gained increasing attention due to its safe operation, environmental friendliness and large-scale application potentials [2-3].

The researches focusing on the optimal scheduling strategies of CAES are growing up increasingly. Look-ahead risk-constrained scheduling of CAES integrated with wind power was studied in [4] where the charging and discharging efficiency was taken as a constant. A hybrid robust-stochastic approach was applied to solve the bidding and offering problems of CAES in the presence of electricity market price uncertainty and carven maximum capacity uncertainty in ref. [5]. A cooptimized CAES dispatch model applying fixed efficiency CAES model was presented in [6] to quantify the arbitrage and reserve revenue in energy and reserve markets. Ref [7] developed a mixed-integer linear programming (MILP) form optimization model for CAES taking part in day-ahead and real-time markets, where the physical characteristics curves of CAES drawn from actual operation was utilized in the modelling. In [8], the benefits of CAES for wind curtailment in multi-area economic dispatch was investigated adopting a risk-based model. A detailed mathematic model of non-supplementary fired CAES with consideration of its thermal and pressure dynamics was established in [9] and further utilized in the optimal dispatch of integrated energy system with CAES-based energy hub. In [10], a short-term economic dispatch model for water-power grids incorporated with AA-CAES was developed in mixed integer non-linear programming (MINLP) formulation. Ref [11] proposed the combined heat and power dispatch model of AA-CAES taking into account of its off-design features.

As stated above, limited studies took into consideration of the part-load conditions when formulating the dispatch model of AA-CAES and few studies described the practical thermodynamic performance of AA-CAES during charging and discharging process. This paper proposes a power system dispatch oriented AA-CAES model considering its accurate physical performance based on the actual experimental data as well as the the detailed temperature and pressure dynamics of storage containers. The nonlinearity of the AA-CAES model is linearized via piecewise linear approximation and special-ordered set of type 2 approaches, and the distribution system dispatch problem is finally cast as a mixed-integer linear program.

The remaining part of this paper is organized as follows. Section 2 presents the modelling of AA-CAES based on the real operation data. Section 3 describes the mathematical formulation of the optimal dispatch of power distribution system integrated with AA-CAES and renewables and its equivalent MILP problem. Section 4 gives the simulation results based on IEEE-33 bus system. The conclusions are drawn in section 5.

2. Modelling of AA-CAES

A typical AA-CAES system was illustrated in figure 1, which is composed of four subsystems including compression train constructed by multi-stage compressors and inter coolers, expansion train consisting of multi-stage expanders and inter-heater, air tank (AT) for storing compressed air and thermal energy storage (TES) for storing high and low temperature heat transfer fluids (HTF).

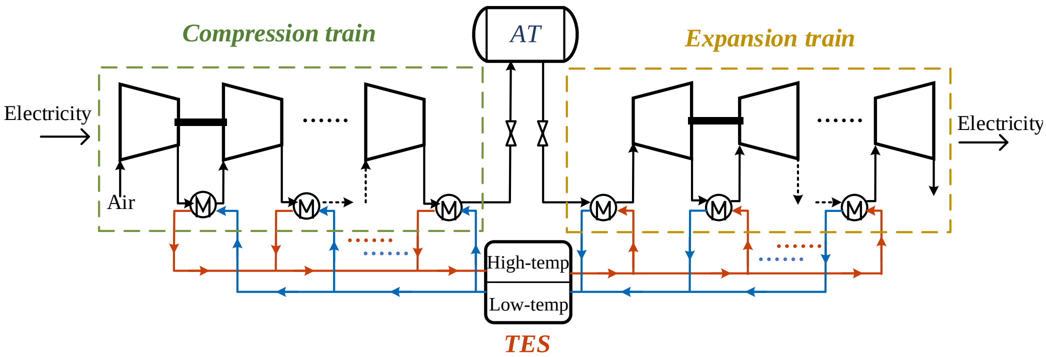

Figure 1. Diagram of typical AA-CAES system.

Due to load fluctuation and energy storage states variation, the compression and expansion train will frequently operate in off-design conditions, where the actual charging and discharging efficiencies deviate from design value. We obtain the physical performance curves of a small-scale AA-CAES from the experiments on compression/expansion train with the rated charging/discharging power of 2 MW, which are depicted in figures 2-3 and will be employed as the inputs of AA-CAES dispatch model after calibration by piece linear functions. The colored lines of figure 2(a) and 2(b) exhibit the stored air mass flow rate (AMFR) and the inlet temperature of high-temperature TES system respectively at given charging power and AT back pressure. Figure 3 illustrates the relationship between released AMFR and discharging power at different temperature level of TES. As seen, the required AMFR per MW power and the inlet temperature of TES depends on the charging/discharging level as well as the storage level of storage containers, additionally, the charging and discharging capacities are also varied from the energy storage states, and are approximately the linear functions of AT temperature and TES temperature respectively.

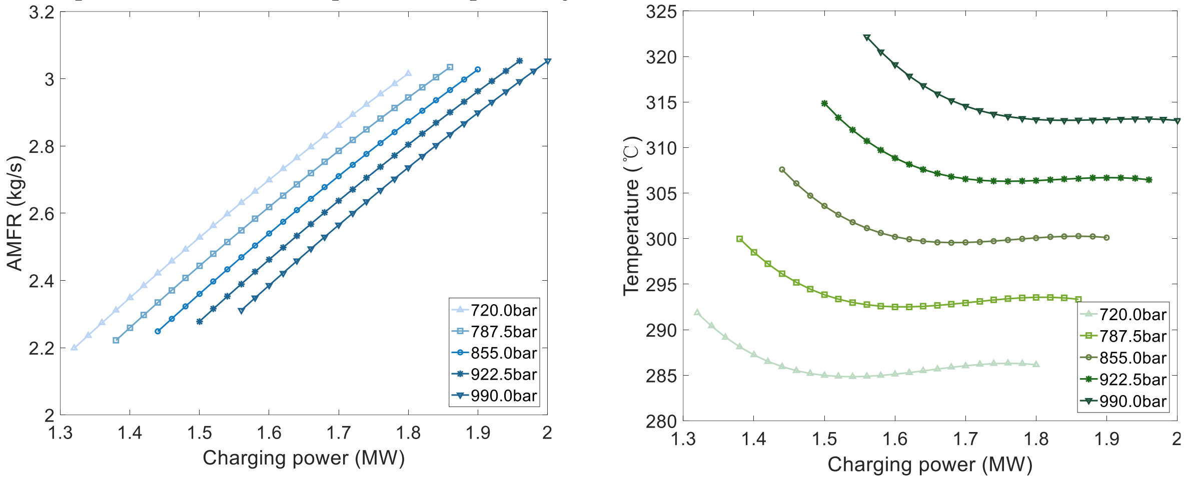

(a) (b)

Figure 2. Compression performance curves of AA-CAES.

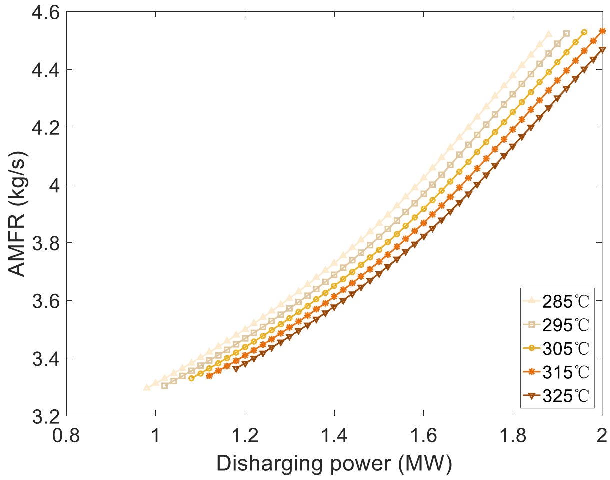

Figure 3. Expansion performance curves of AA-CAES.

Furthermore, the power system dispatch oriented AA-CAES model proposed this paper is constructed by incorporating with the thermodynamic performance curves and takes into consideration of the temperature variation of TES induced by part load charging process. Detailed modelling of AA-CAES is elaborated as follows:

$$0 \le p_{\mathrm{CAESc},t} \le p_{\mathrm{CAESc,max}}, 0 \le p_{\mathrm{CAESd},t} \le p_{\mathrm{CAESd,max}}, \ \forall t \tag{1}$$

$$\mu_{\mathrm{c},t}\left(k_{\mathrm{c1}} p_{\mathrm{AT},t} + b_{\mathrm{c1}}\right) \le p_{\mathrm{CAESc},t} \le \mu_{\mathrm{c},t}\left(k_{\mathrm{c2}} p_{\mathrm{AT},t} + b_{\mathrm{c2}}\right), \ \forall t \tag{2}$$

$$\mu_{\mathrm{d},t}\left(k_{\mathrm{d1}} T_{\mathrm{TES},t} + b_{\mathrm{d1}}\right) \le p_{\mathrm{CAESd},t} \le \mu_{\mathrm{d},t}\left(k_{\mathrm{d2}} T_{\mathrm{TES},t} + b_{\mathrm{d2}}\right), \ \forall t \tag{3}$$

$$\mu_{\mathrm{d},t} + \mu_{\mathrm{c},t} \le 1, \forall t \tag{4}$$

$$p_{\mathrm{AT},t+1}=p_{\mathrm{AT},t}+\alpha\,\mathrm{m_c}\left(p_{\mathrm{AT},t},p_{\mathrm{CAESc},t}\right)-\alpha\,\mathrm{m_d}\left(T_{\mathrm{TES},t},p_{\mathrm{CAESd},t}\right),\ \forall t \tag{5}$$

$$M_{\mathrm{TES},t+1}=M_{\mathrm{TES},t}+\beta_1\,\mathrm{m_c}\left(p_{\mathrm{AT},t},p_{\mathrm{CAESc},t}\right)-\beta_2\,\mathrm{m_d}\left(T_{\mathrm{TES},t},p_{\mathrm{CAESd},t}\right),\ \forall t \tag{6}$$

$$T_{\mathrm{TES},t+1}M_{\mathrm{TES},t}+\beta_1 T_{\mathrm{TES},t+1}\,\mathrm{m_c}\left(p_{\mathrm{AT},t},p_{\mathrm{CAESc},t}\right)=T_{\mathrm{TES},t}M_{\mathrm{TES},t}+\beta_1\,\mathrm{T_{TESin}}\left(p_{\mathrm{AT},t},p_{\mathrm{CAESc},t}\right)\mathrm{m_c}\left(p_{\mathrm{AT},t},p_{\mathrm{CAESc},t}\right),\ \forall t \tag{7}$$

$$\text{Upper and lower bounds of variables} \tag{8}$$

where $p_{\mathrm{CAESc},t}$ and $p_{\mathrm{CAESd},t}$ denote the actual charging and discharging power of AA-CAES, $p_{\mathrm{CAESc,max}}$ and $p_{\mathrm{CAESd,max}}$ represents the rated charging and discharging power. $\mu_{\mathrm{c},t}$ and $\mu_{\mathrm{d},t}$ are binary indicators of charging and discharging states. As indicated in figure 2-3, the upper and lower bounds of charging and discharging power are approximately the linear functions of time-variant air pressure in AT denoted by $p_{\mathrm{AT},t}$ and the temperature in TES represented by $T_{\mathrm{TES},t}$, thus the corresponding linear fitting coefficients k_1~k_4, b_1~b_4 are adopted to describe the state-dependent power capacity. The nonlinear functions $\mathrm{m_c}(\cdot)$, $\mathrm{T_{TESin}}(\cdot)$ and $\mathrm{m_d}(\cdot)$ correspond to the thermodynamic performance curves shown in figure 2(a), 2(b) and figure 3 respectively. The constants α, β_1 and β_2 appearing in (5)-(7) are related to the device parameters of AA-CAES, which is calculated by $\alpha=kR_gT_{\mathrm{AT}}\Delta t/V_{\mathrm{AT}}$, $\beta_1=c_{\mathrm{p,a}}N_{\mathrm{c}}\Delta t/c_{\mathrm{p,HTF}}$ and $\beta_2=c_{\mathrm{p,a}}N_{\mathrm{e}}\Delta t/c_{\mathrm{p,HTF}}$ based on the assumption that the heat capacity of cold and hot fluids though heat exchangers is kept the same, where k denotes the specific heat ratio of air, T_{AT} and V_{AT} are the temperature and volume of AT, R_g is universal gas constant, Δt is the unit scheduling duration, $c_{\mathrm{p,a}}$and $c_{\mathrm{p,HTF}}$ are specific heat capacity of air and heat transfer fluid respectively, N_{c} and N_{e} are the stage number of compression and expansion train, here $N_{\mathrm{c}}=N_{\mathrm{e}}$ in this text and thus $\beta_1=\beta_2$. The power capacity limits and the requirements that charging and discharging is prohibited to take place simultaneously are given by (1)-(4). Constraints (5)-(7) describes the relationships between charging/discharging power and AA-CAES energy storage states evaluated by air pressure of AT, HTF mass stored in TES denoted by $M_{\mathrm{TES},t}$, and the temperature level of TES. The operation ranges of AT and TES are gathered in (8).

3. Economic dispatch of power distribution system

3.1. Model formulation

Assuming no operation cost for AA-CAES and renewable generation due to no need of fuel consumption, the objective function of economic dispatch for power distribution system is to minimize the electricity purchase cost paid to upstream power grid, which is expressed as follows:

$$\min \sum_{t=1}^{24} C_t\, p_{\mathrm{grid},j,t} \tag{9}$$

where C_t is the time-of-use electricity price at period t, and $p_{\mathrm{grid},j,t}$ denotes the electricity bought from external grid connected to the power distribution system at bus j during period t.

The objective function is subjective to the following constraints:

$$P_{ij,t}+p_{\mathrm{W},j,t}+p_{\mathrm{PV},j,t}+p_{\mathrm{CAESd},j,t}+p_{\mathrm{grid},j,t}=\sum_{k\in\pi(j)}P_{jk,t}+p_{\mathrm{L},j,t}+p_{\mathrm{CAESc},j,t},\ \forall l,\ \forall t \tag{10}$$

$$Q_{ij,t}+q_{\mathrm{C},j,t}+q_{\mathrm{grid},j,t}=\sum_{k\in\pi(j)}Q_{jk,t}+q_{\mathrm{L},j,t},\ \forall l,\ \forall t \tag{11}$$

$$V_{j,t}=V_{i,t}-\frac{\left(P_{ij,t}r_{ij}+Q_{ij,t}x_{ij}\right)}{V_0},\ \forall l,\forall t \tag{12}$$

$$W_{j,t}^{\mathrm{l}} \le p_{\mathrm{W},j,t} \le W_{j,t}^{\mathrm{u}},\ \forall j,\ \forall t \tag{13}$$

$$PV_{j,t}^{\mathrm{l}} \le p_{\mathrm{PV},j,t} \le PV_{j,t}^{\mathrm{u}}, \forall j\ , \forall t \tag{14}$$

$$\text{AA-CAES operation constraints (1)-(8)} \tag{15}$$

$$\text{Upper and lower bounds of other variables} \tag{16}$$

where the linearize branch flow model (BFM) [12] is adopted to formulate the power flow constrains for the power distribution system with typical radial topology, which is expressed as (10)-(12), where $P_{ij,t}$ and $Q_{ij,t}$ are the active and reactive power though line $l(ij)$, $q_{\mathrm{grid},j,t}$ and $q_{\mathrm{C},j,t}$ represent the reactive power supplied by upstream grid and continously adjustable reactive compenators equipped at bus j, $p_{\mathrm{L},j,t}$ and $q_{\mathrm{L},j,t}$ denote the active and reactive load demands at bus j, $V_{j,t}$ and V_0 are the nodal voltage magnitudes at bus j and the reference bus, r_{ij} and x_{ij} are the resistance and reactance of line $l(ij)$, $p_{\mathrm{W},j,t}$ and $p_{\mathrm{PV},j,t}$ are the wind and photovoltaic (PV) outputs located at bus j during period t, which are limited within the output constraints given by (13)-(14) respectively. $W_{j,t}^{\mathrm{l}}$, $W_{j,t}^{\mathrm{u}}$, $PV_{j,t}^{\mathrm{l}}$ and $PV_{j,t}^{\mathrm{u}}$ are the available wind power and PV output bounds determined by the forecast output curves. Upper and lower bounds of other variables are collected in (16).

3.2. Model simplifications

To sum up, the optimal dispatch of power distribution system integrated with AA-CAES, wind and PV plant can be formulated as MINLP, which is given by:

$$\begin{aligned} &\min \ \sum_{t=1}^{24} C_t\, p_{\mathrm{grid},\,j,t} \\ &\text{s.t.} \quad \text{(1)-(8), (10)-(14), (16)} \end{aligned} \tag{17}$$

where constraints (2)-(3), (5)-(7) contain non-linear terms. The binary-continuous product term in the form of $z{=}xy$, e.g. (2)-(3), where y is a binary variable and the continuous variable x is limited within the ranges $[\underline{x},\ \overline{x}]$ can be linearized as [13]:

$$\underline{x}y \le z \le \overline{x}y,\ \ \underline{x}(1-y) \le x - z \le \overline{x}(1-y) \tag{18}$$

Piecewise linear approximation and special-ordered set of type 2 approaches [13-14] are adopted to tackle with the nonlinear functions describing AA-CAES thermodynamic performances shown in (5)-(7). Considering a bivariate continuous nonlinear function $\mathrm{f}(x, y)$, positive weight coefficient variables λ_{mn} are induced for each grid point (x_n, y_m), and thus any point in the feasible region can be represented as

$$x = \sum_{m=0}^{M}\sum_{n=0}^{N} \lambda_{mn} x_n,\ y = \sum_{m=0}^{M}\sum_{n=0}^{N} \lambda_{mn} y_m \tag{19}$$

$$\sum_{m=0}^{M}\sum_{n=0}^{N} \lambda_{mn} = 1,\ \lambda_{mn} \ge 0 \tag{20}$$

with the function value at that point calculated by

$$\mathrm{f}\,(x, y) = \sum_{m=0}^{M}\sum_{n=0}^{N} \lambda_{mn} y_{mn} \tag{21}$$

IOP Conf. Series: Earth and Environmental Science **529** (2020) 012006 doi:10.1088/1755-1315/529/1/012006

Additionally, the marginal weight vectors from *x*-perspective $\lambda_n = \sum_{m=0}^{M} \lambda_{mn}$ and that from *y*-viewpoint $\lambda_m = \sum_{n=0}^{N} \lambda_{mn}$ satisfy the special ordered set of type two (SOS_2) requirements, which means at most two adjacent elements of λ_n and λ_m can be positive. As for the constraint describing the temperature dynamics shown in (7), it contains four bi-linear terms, each of which can be further linearized based on the abovementioned method. Finally, the non-linear dispatch model given in (17) is converted into MILP problem and can be effectively solved by commercial solvers.

4. Case study

4.1. System settings

The revised IEEE 33-bus test system with AA-CAES interconnected at bus 6 is shown in figure 4, which also consists of a 12 MW distributed wind plant, a 3 MW PV plant and a static var generator (SVG) with the capacity of 2 MVar. Time-of-use electricity price are shown in figure 5 and the hourly load, wind and PV output forecast curves are depicted in figure 6.

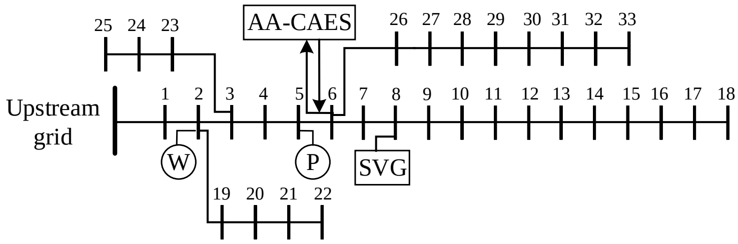

Figure 4. Modified IEEE 33-bus system.

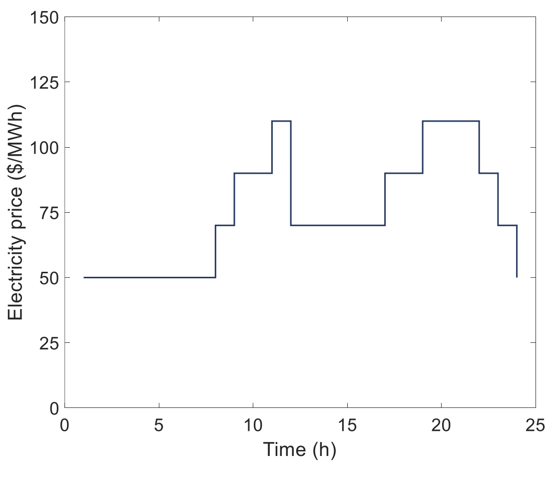

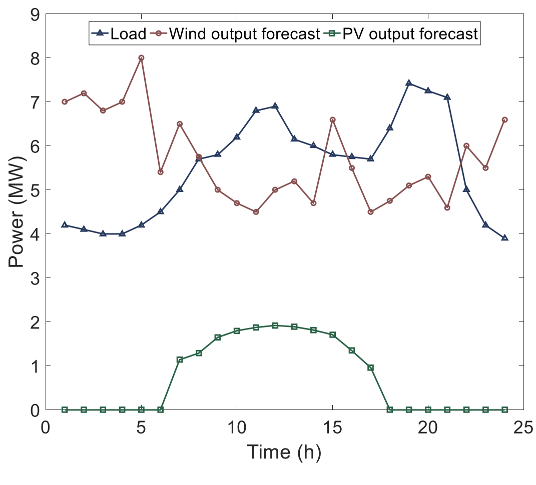

Figure 5. Time-of-use electricity price.

Figure 6. Load, wind and PV output forecast.

4.2. Simulation results

The generation scheduling results of AA-CAES is exhibited in figure 7. Figure 8 illustrates the temperature variation in TES as well as the air pressure change in AT. Optimal scheduling of wind and PV output is given in figure 9 and figure 10 respectively. As seen, AA-CAES mostly charges during valley hours consuming the redundant wind power and discharges in peak hours. The excess PV outputs during the 7th and 11th periods are made use of for air compression. It can be observed from figure 8 that there is an appreciable variation of temperature within a day, the overall temperature difference amounting to 21.5 ℃, giving rise to the maximum change of released AMFR per MW power by nearly 40%, which indicates the necessity to take into consideration of the temperature variation in TES. Besides, the HTF mass stored in TES and the air pressure of AT will theoretically change parasynchronously when compression and expansion stages are equivalent and the thermal capacity of air and THF is identical.

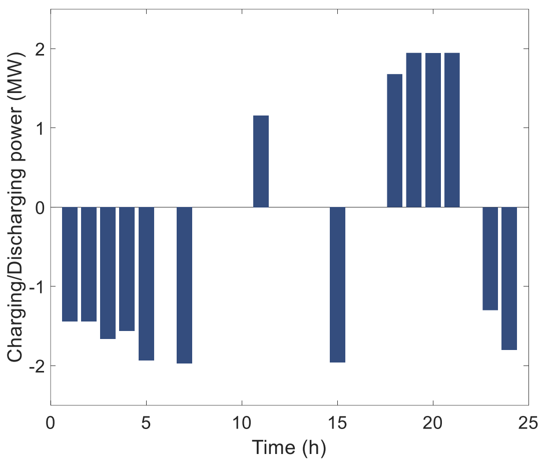

Figure 7. Scheduling results of AA-CAES.

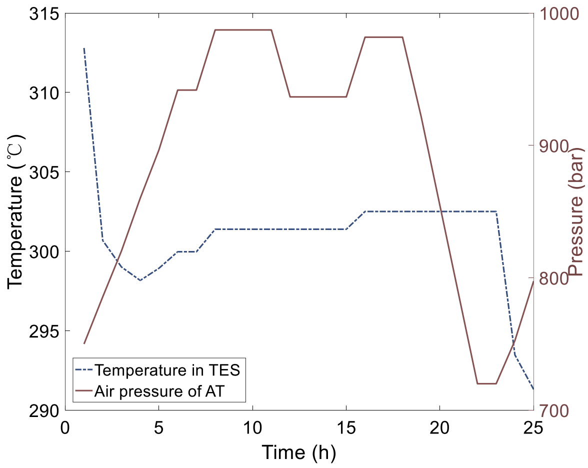

Figure 8. Temperature and pressure dynamics of AA-CAES.

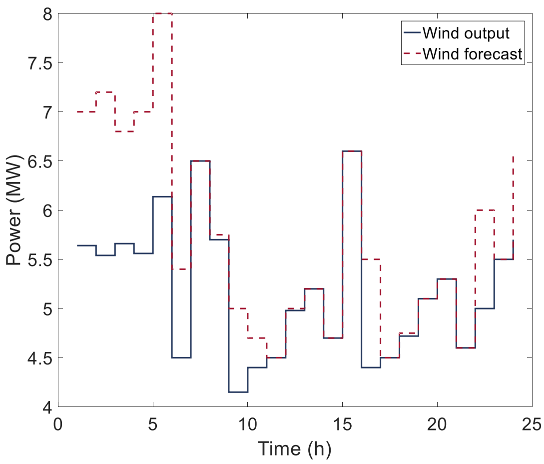

Figure 9. Scheduling results of wind plant.

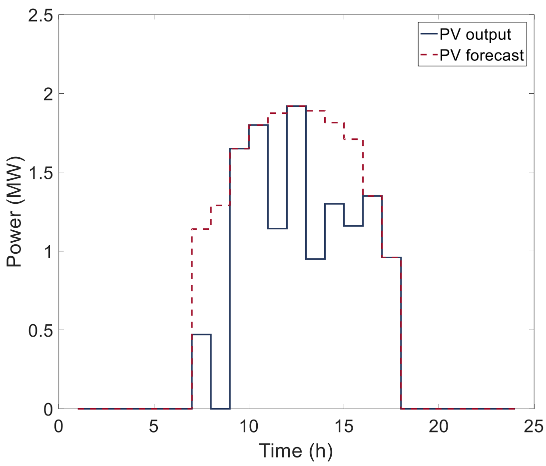

Figure 10. Scheduling results of PV plant.

We compare the scheduling results of power distribution system with and without AA-CAES, as given in table. 1. It shows an apparent 45.3% reduction of the total renewables shedding and 87.2% decrease of the total operation cost, which indicates the significant effect of AA-CAES for peak shaving, valley levitating and renewables accommodation.

Table 1. Comparison of the dispatch results with and without AA-CAES

Scenarios	Wind shedding (MWh)	PV shedding (MWh)	Total renewables shedding (MWh)	Total cost ($)
With AA-CAES	12.61	4.70	17.31	123.45
Without AA-CAES	31.62	0.00	31.62	961.55

The scheduling results following simple dispatch model of AA-CAES with fixed efficiency and constant temperature in TES are shown in figure 11 and figure 12. It can be seen that the charging and discharging power is often outside their adjustable ranges. Moreover, the pressure variation obtained from fixed efficiency model deviates from its actual trend especially during discharging process. We can observe from figure 12 that the air pressure at the beginning of the 22th period is 659.3 bar, which is 8.4% lower than the permitted minimum working pressure of air tank. In conclusion, the neglecting of the actual physical performance of AA-CAES results in misestimating of energy storage level and infeasible scheduling strategies as well.

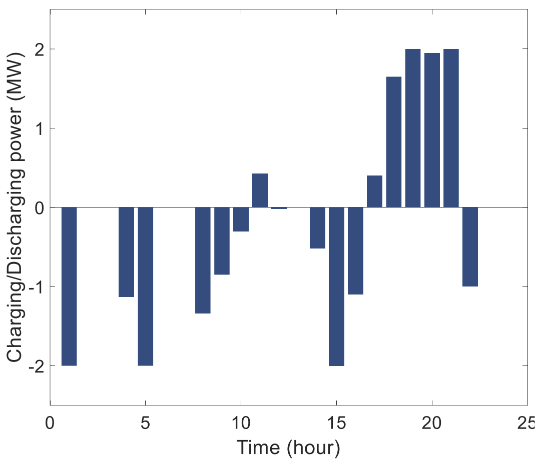

Figure 11. AA-CAES schedule obtained from fixed efficiency model.

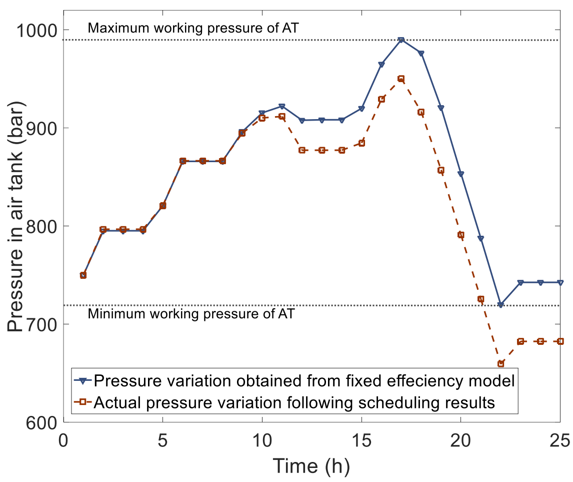

Figure 12. Pressure variation in air tank obtained from fixed efficiency model.

5. Conclusion

A measurement-driven power-system-dispatch-oriented AA-CAES model with consideration of its actual thermodynamic performance under off-design conditions is proposed and further incorporated with the economic dispatch problem of power distribution system with renewable generations. Because the performance curves of AA-CAES are obtained from actual operation data, the practicability of the dispatch model is guaranteed and the authenticity of the scheduling results is reliable. Multidimensional piecewise linear approximation and special-ordered set of type 2 approaches are adopted to formulate its equivalent MILP problem. Case studies demonstrate the benefits of AA-CAES for renewables accommodation, peak shaving and system operation costs reduction, and verifies the necessity to take into consideration of the actual physical performance of AA-CAES, which otherwise gives rise to infeasible scheduling strategies.

References

[1] Buonomano A, Calise F, D'accadia M D and Vicidomini M 2018 A hybrid renewable system based on wind and solar energy coupled with an electrical storage: dynamic simulation and economic assessment *Energy* **155** 174-89
[2] Han Z, Guo S 2018 Investigation of operation strategy of combined cooling, heating and power (CCHP) system based on advanced adiabatic compressed air energy storage *Energy* **160** 290-308
[3] Becattini V, Geissbühler L, Zanganeh G, Haselbacher A and Steinfeld A 2018 Pilot-scale demonstration of advanced adiabatic compressed air energy storage, part 2: tests with combined sensible/latent thermal-energy storage *Journal of Energy Storage* **17** 140-52
[4] Aliasghari P, Zamani-Gargari M, Mohammadi-Ivatloo B 2018 Look-ahead risk-constrained scheduling of wind power integrated system with compressed air energy storage (CAES) plan *Energy* **160** 668-77
[5] Cai W, Mohammaditab R, Fathi G, Wakil K, Ebadi A G and Ghadimi N 2019 Optimal bidding and offering strategies of compressed air energy storage: a hybrid robust-stochastic approach *Renew. Energ.* **143** 1-8

IOP Conf. Series: Earth and Environmental Science **529** (2020) 012006 doi:10.1088/1755-1315/529/1/012006

[6] Drury E, Denholm P, Sioshansi R 2011 The value of compressed air energy storage in energy and reserve markets *Energy* **36** 4959-73

[7] Khatami R, Oikonomou K, Parvania M 2019 Look-ahead optimal participation of compressed air energy storage in day-ahead and real-time markets *IEEE Transactions on Sustainable Energy*

[8] Azizivahed A, Razavi S E, Arefi A, Ghadi M J, Li L, Zhang J, Shafie-khah M and Catalao J P S 2019 Risk-oriented multi-area economic dispatch solution with high penetration of wind power generation and compressed air energy storage system *IEEE Transactions on Sustainable Energy*

[9] Li R, Chen L, Yuan T and Li C 2016 Optimal dispatch of zero-carbon-emission micro energy internet integrated with non-supplementary fired compressed air energy storage system *Journal of Modern Power Systems and Clean Energy* **4** 566-80

[10] Jabari F, Ivatloo B M, Sharifian M B B and Ghaebi H 2019 Day-ahead economic dispatch of coupled desalinated water and power grids with participation of compressed air energy storages *Journal of Operation and Automation in Power Engineering* **7** 40-8

[11] Li Y, Miao S, Yin B, Han J, Zhang S, Wang J and Luo X 2019 Combined heat and power dispatch considering advanced adiabatic compressed air energy storage for wind power accommodation *Energy Convers. Manage.* **200** 112091

[12] Wang S, Chen S, Ge L and Wu L 2016 Distributed generation hosting capacity evaluation for distribution systems considering the robust optimal operation of OLTC and SVC *IEEE Transactions on Sustainable Energy* **7** 1111-23

[13] Wei W and Wang J 2020 *Modeling and Optimization of Interdependent Energy Infrastructures* (Cham: Springer) pp 509-536

[14] Correa-Posada C M, Sánchez-Martín P 2014 Gas network optimization: A comparison of piecewise linear models *Optimization Online*

Acknowledgments

This work is supported by State Grid Anhui Electric Power Co., Ltd. Science and Technology Project “Research on grid-connected operation control and market mechanism of compressed air energy storage” (521205180021).